Twist-3 gluon contribution to Sivers asymmetry in J/ψ production in semi-inclusive deep inelastic scattering

Longjie Chen,[*] Hongxi Xing,[†] and Shinsuke Yoshida[‡]

Key Laboratory of Atomic and Subatomic Structure and Quantum Control (MOE), Institute of Quantum Matter, South China Normal University, Guangzhou 510006, China; Guangdong Provincial Key Laboratory of Nuclear Science, Institute of Quantum Matter, South China Normal University, Guangzhou 510006, China; and Guangdong-Hong Kong Joint Laboratory of Quantum Matter, Southern Nuclear Science Computing Center, South China Normal University, Guangzhou 510006, China

(Received 25 June 2023; accepted 18 August 2023; published 14 September 2023)

We carry out the first calculation for the twist-3 gluon contribution to the single transverse-spin asymmetry (SSA) in J/ψ production in semi-inclusive deep inelastic scattering. Our result shows that the J/ψ SSA is an ideal observable to pin down the C-even type twist-3 gluon distribution that has a direct relationship with the gluon transverse-momentum-dependent distribution function. We also perform some numerical simulations of the J/ψ SSA for the kinematics accessible at the future electron-ion-collider experiment. For color-singlet contribution, the hadronization effect of J/ψ is completely canceled at the level of the SSA, and the spin-dependent structure functions directly reflect the behavior of the C-even twist-3 gluon distribution.

DOI: 10.1103/PhysRevD.108.054021

I. INTRODUCTION

The investigation of the nucleon internal structure in high energy scatterings has been one of the central subjects in basic science since quantum chromodynamics (QCD) was established as a fundamental theory of the strong interaction. A lot of knowledge has been accumulated in the past half century through the perturbative QCD analysis of experimental data. However, in spite of tremendous theoretical and experimental effort, a lot of mysteries still lie in the nucleon structure. In particular, the role of gluons inside the nucleon is leaving a lot of room for research. The investigation of the gluon spin structure is one of the main subjects of the experiment at Relativistic Heavy Ion Collider (RHIC) that was launched in 2000. The evaluation of the gluon spin contribution to the proton spin is a major progress that was made in the past couple of decades [1,2]. Further investigation will be inherited by the next-generation collider experiment, Electron Ion Collider (EIC) [3]. The EIC experiment aims to understand deeper gluon structure like the three-dimensional orbital motion of gluons inside the proton. The importance of the orbital motions of the partons was realized by the emergence of the large single transverse-spin asymmetry (SSA) in high energy hadron scatterings. The large SSA was first observed in the late ’70s [4,5], and it turned out that the conventional parton picture could not describe it at all. The observation of the large SSA motivated the improvement of the conventional perturbative QCD framework. The transverse-momentum-dependent (TMD) factorization is known as one of the successful frameworks in describing existing data of the SSA. The nonperturbative functions in the TMD factorization represent the three-dimensional motion of the partons, and the success of this framework made us realize the importance of the orbital motions of the partons. Another successful framework is the twist-3 contributions in the collinear factorization. This framework describes incoherent multiparton scattering in a hard process, and this is successful in describing SSAs in single-scale processes like $pp \to \pi X$ measured at RHIC. Although these two frameworks basically have different applicable conditions, it was found that there is a marginal region where both frameworks are valid in some processes [6–11]. The equivalence of two frameworks is important for giving a unified picture to the origin of the SSA.

Heavy flavored hadron productions are important in the context of the investigation of the gluon structure because the heavy quark fragmenting into a final state hadron is

[*]chenlongjieusc@163.com
[†]hxing@m.scnu.edu.cn
[‡]shinyoshida85@gmail.com

mainly produced by a fusion of gluon inside the proton [12]. The SSA in the heavy flavored hadron production is one of ideal observables to investigate the orbital motions of gluons. Those SSAs have been well discussed based on the TMD factorization for D-meson production [13–17] and J/ψ production [15,17–25]. On the other hand, the twist-3 gluon contribution to the SSA has been calculated only for D-meson production [26–30]. In this paper, we carry out the first calculation for the twist-3 gluon contribution to the SSA in J/ψ production in semi-inclusive deep inelastic scattering (SIDIS). This is required to deal with the data of the J/ψ SSA in a full kinematic range of the EIC experiment together with the TMD framework and give a unified interpretation to the data. We will also perform some numerical simulations for the J/ψ SSA. Our result clarifies the role of the J/ψ SSA in the determination of the twist-3 gluon distribution function that could give indirect information about the orbital motion of the gluons inside the proton.

The remainder of this paper is organized as follows: In Sec. II, we introduce definitions of the twist-3 gluon distribution functions relevant to our study and show some relations among them. In Sec. III, we introduce the frame we will work on and show our derivation of the twist-3 cross section formula in detail. In Sec. IV, we show some numerical simulations with simple models for the normalized structure functions that are accessible at the EIC. Section V is devoted to a summary of our study.

II. DEFINITIONS OF TWIST-3 GLUON DISTRIBUTION FUNCTIONS

In this section, we recall the definitions of the twist-3 gluon distribution functions relevant to our study. Two types of the twist-3 functions, the kinematical functions and the dynamical functions, in general contribute to the SSA. The kinematical functions of the transversely polarized proton are defined as follows [31]:

$$\begin{aligned}\Phi_\partial^{\alpha\beta\gamma}(x) &= \int \frac{d\lambda}{2\pi} e^{i\lambda x}\langle pS_\perp|F^{\beta n}(0)F^{\alpha n}(\lambda n)|pS_\perp\rangle(i\overleftarrow{\partial}^\gamma_\perp)\\
&\equiv \lim_{\xi_\perp\to 0}\int \frac{d\lambda}{2\pi} e^{i\lambda x}\langle pS_\perp|\Big(F^{\beta n}(0)[0,\infty n]\Big)_a i\frac{d}{d\xi_{\perp\gamma}}\Big([\infty n+\xi_\perp,\lambda n+\xi_\perp]F^{\alpha n}(\lambda n+\xi_\perp)\Big)_a|pS_\perp\rangle\\
&= \frac{M_N}{2}g_\perp^{\alpha\beta}\epsilon^{pnS_\perp\gamma}G_T^{(1)}(x) + i\frac{M_N}{2}\epsilon^{pn\alpha\beta}S_\perp^\gamma\Delta G_T^{(1)}(x) + \frac{M_N}{8}\Big(\epsilon^{pnS_\perp\{\alpha}g_\perp^{\beta\}\gamma} + \epsilon^{pn\gamma\{\alpha}S_\perp^{\beta\}}\Big)\Delta H_T^{(1)}(x) + \cdots, \qquad (1)\end{aligned}$$

where $p, S_\perp$, and M_N are the proton's momentum, spin, and mass, respectively. We used the simplified notation $\epsilon^{pnS_\perp\gamma} = \epsilon^{\mu\nu\rho\gamma}p_\mu n_\nu S_{\perp\rho}$. $[0,\lambda n]$ denotes the gauge-link operator,

$$[0,\lambda n] \equiv \mathrm{P}\exp\left(ig\int_\lambda^0 dt A^n(tn)\right), \qquad (2)$$

which guarantees the gauge-invariance of the matrix element. n is a lightlike vector that satisfies $p\cdot n = 1$, $n^2 = 0$. One can find that the above matrix element has the relationship with the gluon TMD matrix element $\Gamma^{ij}(x,k_T)$ defined in Eq. (12) in [32] as

$$\Phi_\partial^{\alpha\beta\gamma}(x) = -\frac{M_N}{p^+}\int d^2k_T k_T^\gamma \Gamma^{\beta\alpha}(x,k_T), \qquad (3)$$

which gives the relations between the kinematical functions and the gluon TMD functions defined in [32] as

$$F^{(1)}(x) = \frac{x}{2M_N^2}\int d^2k_T \mathbf{k}_T^2 F(x,\mathbf{k}_T^2) \quad (F = G_T, \Delta G_T, \Delta H_T). \qquad (4)$$

The superscript "(1)" of a kinematical function denotes the first $\mathbf{k}_T^2$-moment of the corresponding gluon TMD function. A naively T-odd observable like the SSA receives the contributions from $G_T^{(1)}(x)$ and $\Delta H_T^{(1)}(x)$.

The dynamical gluon distribution functions are defined by a matrix element composed of three gluon field strength tensors [28,33]. The dynamical functions are categorized into two types, C-even function $N(x_1,x_2)$ and C-odd function $O(x_1,x_2)$, reflecting the fact that there are two structure constants if^{abc} and d^{abc} in SU(N_c) group,

$$\begin{aligned}N^{\alpha\beta\gamma}(x_1,x_2) &= i\int\frac{d\lambda}{2\pi}\int\frac{d\mu}{2\pi}e^{i\lambda x_1}e^{i\mu(x_2-x_1)}\langle pS_\perp|if^{bca}F_b^{\beta n}(0)gF_c^{\gamma n}(\mu n)F_a^{\alpha n}(\lambda n)|pS_\perp\rangle\\
&= 2iM_N\Big[g_\perp^{\alpha\beta}\epsilon^{\gamma pnS_\perp}N(x_1,x_2) - g_\perp^{\beta\gamma}\epsilon^{\alpha pnS_\perp}N(x_2,x_2-x_1) - g_\perp^{\alpha\gamma}\epsilon^{\beta pnS_\perp}N(x_1,x_1-x_2)\Big] + \cdots, \qquad (5)\end{aligned}$$

$$O^{\alpha\beta\gamma}(x_1,x_2) = i\int\frac{d\lambda}{2\pi}\int\frac{d\mu}{2\pi}e^{i\lambda x_1}e^{i\mu(x_2-x_1)}\langle pS_\perp|d^{bca}F_b^{\beta n}(0)gF_c^{\gamma n}(\mu n)F_a^{\alpha n}(\lambda n)|pS_\perp\rangle$$
$$= 2iM_N\left[g_\perp^{\alpha\beta}\epsilon^{\gamma pnS_\perp}O(x_1,x_2) + g_\perp^{\beta\gamma}\epsilon^{\alpha pnS_\perp}O(x_2,x_2-x_1) + g_\perp^{\alpha\gamma}\epsilon^{\beta pnS_\perp}O(x_1,x_1-x_2)\right] + \cdots, \quad (6)$$

where we omitted gauge links for simplicity. These dynamical functions have the following symmetries:

$$O(x_1,x_2) = O(x_2,x_1), \qquad O(x_1,x_2) = O(-x_1,-x_2),$$
$$N(x_1,x_2) = N(x_2,x_1), \qquad N(x_1,x_2) = -N(-x_1,-x_2). \quad (7)$$

The kinematical functions and the C-even function $N(x_1,x_2)$ are not independent of each other. The following relations were derived in [31]:

$$G_T^{(1)}(x) = -4\pi(N(x,x) - N(x,0)),$$
$$\Delta H_T^{(1)}(x) = 8\pi N(x,0). \quad (8)$$

They show the relationships between the first $\mathbf{k}_T^2$-moment of the gluon Sivers function and the C-even twist-3 gluon distribution function in analogy with the relationship between the twist-3 Qiu-Sterman function and the quark Sivers function [34,35].

III. CALCULATION OF THE SSA IN J/ψ PRODUCTION IN SIDIS

A. Unpolarized cross section for J/ψ production in SIDIS

We calculate the SSA in J/ψ production in SIDIS,

$$e(\ell) + p^\uparrow(p,S_\perp) \to e(\ell') + J/\psi(P_{J/\psi}) + X, \quad (9)$$

in the hadron frame [36]. It is convenient to use the following Lorentz invariant variables to express a cross section formula in SIDIS:

$$S_{ep} = (p+\ell)^2, \qquad Q^2 = -q^2 = -(\ell-\ell')^2,$$
$$x_B = \frac{Q^2}{2p\cdot q}, \qquad z_f = \frac{p\cdot P_{J/\psi}}{p\cdot q}. \quad (10)$$

All momenta and the spin vector of the polarized proton are given in this frame as

$$p = \left(\frac{Q}{2x_B},0,0,\frac{Q}{2x_B}\right), \qquad q = (0,0,0,-Q),$$
$$P_{J/\psi} = \frac{z_f Q}{2}\left(1+\frac{P_T^2}{Q^2}+\frac{m_{J/\psi}^2}{z_f^2Q^2}, \frac{2P_T}{Q}\cos\chi, \frac{2P_T}{Q}\sin\chi, -1+\frac{P_T^2}{Q^2}+\frac{m_{J/\psi}^2}{z_f^2Q^2}\right),$$
$$S_\perp = (0,\cos\Phi_S,\sin\Phi_S,0), \quad (11)$$

where $P_T = |P_{J/\psi}^\perp|/z_f$, and $m_{J/\psi}$ is the mass of J/ψ. Using these variables, the cross section formula is given by

$$\frac{d^6\sigma}{dx_BdQ^2dz_fdP_T^2d\phi d\chi} = \frac{\alpha_{em}^2}{128\pi^4S_{ep}^2x_B^2Q^2}z_fL_{\mu\nu}(\ell,\ell')W^{\mu\nu}(p,q,P_{J/\psi}), \quad (12)$$

where $\alpha_{em} = e^2/4\pi$ is the QED coupling constant, Φ_S, χ, and ϕ are the azimuthal angles of the proton's spin, the hadron plane, and the lepton plane, respectively, as shown in Fig. 1, and the leptonic tensor is given by $L_{\mu\nu}(\ell,\ell') = 2(\ell_\mu\ell'_\nu + \ell_\nu\ell'_\mu) - Q^2g^{\mu\nu}$. The hadronic tensor $W_{\mu\nu}(p,q,P_{J/\psi})$ describes the scattering between the virtual photon and the proton and the hadronization process of the charm quark pair into J/ψ. We adopt nonrelativistic QCD (NRQCD) framework [37,38] for the description of the hadronization mechanism of J/ψ. Within NRQCD, the J/ψ production is illustrated as

$$e(\ell) + p(p) \to e(\ell') + \sum_n c\bar{c}[n](P_{J/\psi}) + X, \quad (13)$$

where $n = {}^3S_1^{[1]}, {}^1S_0^{[8]}, {}^3S_1^{[8]}, \cdots$ denotes possible Fock states of the charm quark pair hadronizing into J/ψ. In this paper, we focus on the color singlet contribution ${}^3S_1^{[1]}$ as the first attempt to calculate the twist-3 gluon distribution effect on the J/ψ SSA. The color-singlet hadronization gives the following structure in the spinor space:

$$\mathcal{N}\langle\mathcal{O}^{J/\psi}({}^3S_1^{[1]})\rangle\not{\epsilon}(\not{P}_{J/\psi}+m_{J/\psi}),$$
$$\sum\epsilon^\rho\epsilon^{*\sigma} = -g^{\rho\sigma} + \frac{P_{J/\psi}^\rho P_{J/\psi}^\sigma}{m_{J/\psi}^2}, \quad (14)$$

where $\langle\mathcal{O}^{J/\psi}({}^3S_1^{[1]})\rangle$ is the long distance matrix element (LDME) that represents the hadronization effect of the

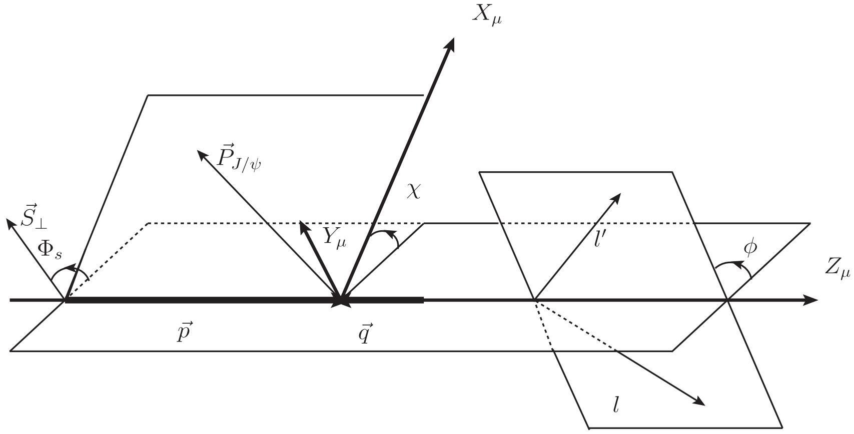

FIG. 1. Schematic illustration of the scattering in the hadron frame.

charm quark pair with the quantum state ${}^3S_1^{[1]}$ into J/ψ. We don't need the explicit form of the normalization factor $\mathcal{N}$ in our study because it is completely canceled at the level of the SSA that is given by the ratio of two cross sections. For the unpolarized cross section, the hadronic tensor is given by

$$W^{\mu\nu}(p,q,P_{J/\psi}) = \int_0^1 \frac{dx}{x} G(x) \langle \mathcal{O}^{J/\psi}({}^3S_1^{[1]}) \rangle w^{\mu\nu}(xp,q,P_{J/\psi}), \tag{15}$$

where $G(x)$ is the unpolarized gluon distribution function, and $w^{\mu\nu}(xp,q,P_{J/\psi})$ represents the hard scattering between the virtual photon and a parton inside the proton. We can calculate $L^{\mu\nu}(\ell,\ell')w^{\mu\nu}(xp,q,P_{J/\psi})$ perturbatively by considering the diagrams in the leading order (LO) with respect to the strong coupling constant for the unpolarized cross section. The hadronic tensor $W_{\mu\nu}(p,q,P_{J/\psi})$ is conventionally expanded in terms of nine independent tensors $\mathcal{V}_i^{\mu\nu}$ $(i = 1,2,\ldots 9)$ [36] as

$$W^{\mu\nu} = \sum_{i=1}^{9} (W^{\rho\sigma}\tilde{\mathcal{V}}_{i\rho\sigma})\mathcal{V}_i^{\mu\nu}, \tag{16}$$

where the inverse tensors $\tilde{\mathcal{V}}_{i\rho\sigma}$ satisfy $\mathcal{V}_i^{\mu\nu}\tilde{\mathcal{V}}_{i'\mu\nu} = \delta_{ii'}$. Here, we just show the explicit definitions of the symmetric tensors that are relevant to our study:

$$\mathcal{V}_1^{\mu\nu} = X^\mu X^\nu + Y^\mu Y^\nu, \qquad \mathcal{V}_2^{\mu\nu} = g^{\mu\nu} + Z^\mu Z^\nu, \qquad \mathcal{V}_3^{\mu\nu} = T^\mu X^\nu + X^\mu T^\nu,$$
$$\mathcal{V}_4^{\mu\nu} = X^\mu X^\nu - Y^\mu Y^\nu, \qquad \mathcal{V}_8^{\mu\nu} = T^\mu Y^\nu + Y^\mu T^\nu, \qquad \mathcal{V}_9^{\mu\nu} = X^\mu Y^\nu + Y^\mu X^\nu,$$
$$\tilde{\mathcal{V}}_1^{\mu\nu} = \frac{1}{2}(2T^\mu T^\nu + X^\mu X^\nu + Y^\mu Y^\nu), \qquad \tilde{\mathcal{V}}_2^{\mu\nu} = T^\mu T^\nu, \qquad \tilde{\mathcal{V}}_3^{\mu\nu} = -\frac{1}{2}(T^\mu X^\nu + X^\mu T^\nu),$$
$$\tilde{\mathcal{V}}_4^{\mu\nu} = \frac{1}{2}(X^\mu X^\nu - Y^\mu Y^\nu), \qquad \tilde{\mathcal{V}}_8^{\mu\nu} = -\frac{1}{2}(T^\mu Y^\nu + Y^\mu T^\nu), \qquad \tilde{\mathcal{V}}_9^{\mu\nu} = \frac{1}{2}(X^\mu Y^\nu + Y^\mu X^\nu),$$

where each vector is defined by

$$T^\mu = (1,0,0,0), \qquad X^\mu = (0,\cos\chi,\sin\chi,0), \qquad Y^\mu = (0,-\sin\chi,\cos\chi,0), \qquad Z^\mu = (0,0,0,1). \tag{17}$$

Then we can calculate $L_{\mu\nu}W^{\mu\nu}$ as

$$L_{\mu\nu}W^{\mu\nu} = \sum_{i=1,\ldots,4,8,9} [L_{\mu\nu}\mathcal{V}_i^{\mu\nu}][W_{\rho\sigma}\tilde{\mathcal{V}}_i^{\rho\sigma}] = Q^2 \sum_{i=1,\ldots,4,8,9} \mathcal{A}_i(\phi-\chi)[W_{\rho\sigma}\tilde{\mathcal{V}}_i^{\rho\sigma}], \tag{18}$$

where the azimuthal dependences $\mathcal{A}_i(\varphi)$ are given by

$$\mathcal{A}_1(\varphi) = \frac{4}{y^2}\left(1 - y + \frac{y^2}{2}\right), \qquad \mathcal{A}_2(\varphi) = -2, \qquad \mathcal{A}_3(\varphi) = -\frac{4}{y^2}(2-y)\sqrt{1-y}\cos\varphi,$$
$$\mathcal{A}_4(\varphi) = \frac{4}{y^2}(1-y)\cos 2\varphi, \qquad \mathcal{A}_8(\varphi) = -\frac{4}{y^2}(2-y)\sqrt{1-y}\sin\varphi, \qquad \mathcal{A}_9(\varphi) = \frac{4}{y^2}(1-y)\sin 2\varphi, \tag{19}$$

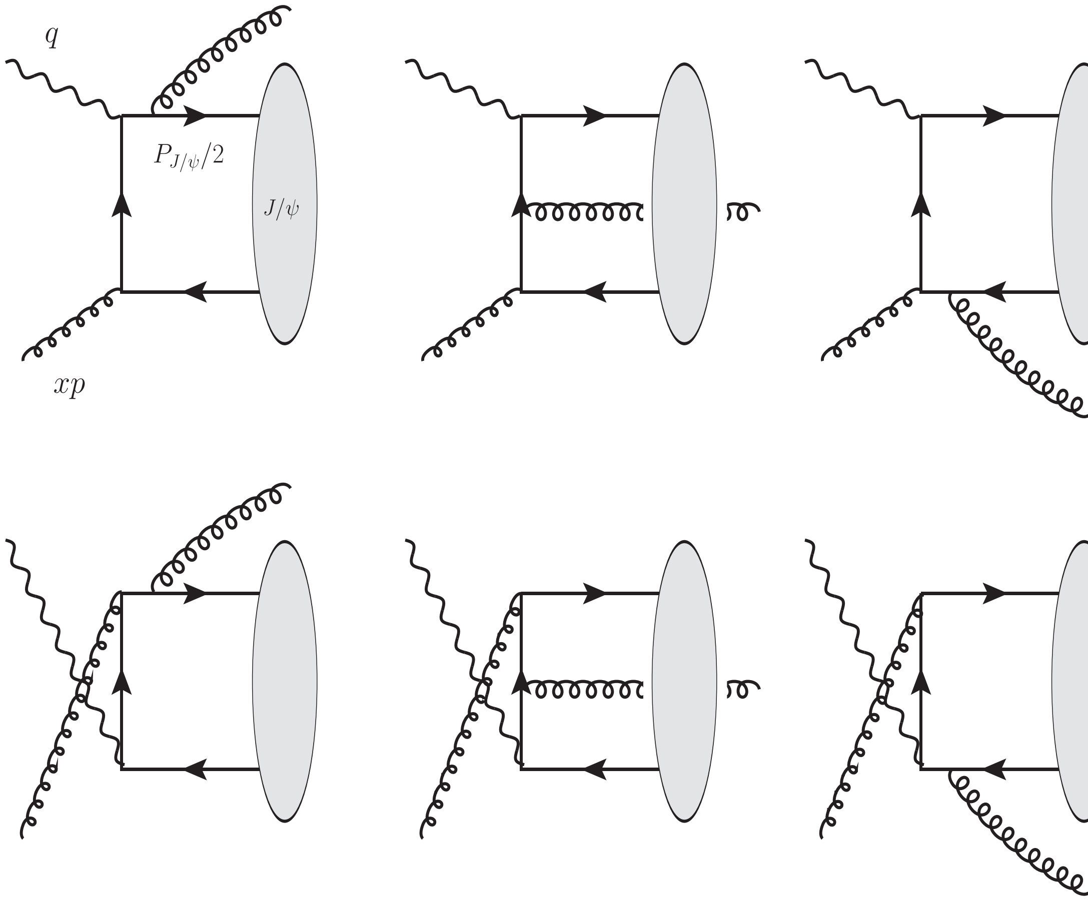

FIG. 2. Diagrams that contribute to the unpolarized cross section. $w^{\mu\nu}(xp, q, P_{J/\psi})$ is given by the squared amplitude of the sum of these six diagrams.

where $y = \frac{Q^2}{x_B S_{ep}}$. We can derive the unpolarized cross section formula by computing all the diagrams in Fig. 2 as

$$\frac{d^6\sigma}{dx_B dQ^2 dz_f dP_T^2 d\phi d\chi} = \frac{\alpha_{em}^2 \alpha_s^2 e_c^2}{4\pi S_{ep}^2 x_B^2 Q^2} (\mathcal{N}\langle \mathcal{O}^{J/\psi}(^3S_1^{[1]})\rangle) \sum_{i=1,\ldots,4,8,9} \mathcal{A}_i(\phi-\chi) \int_0^1 \frac{dx}{x} G(x)\hat{\sigma}_i \times \delta\left[\frac{P_T^2}{Q^2} - \left(1 - \frac{1}{\hat{x}} + \frac{m_{J/\psi}^2}{z_f Q^2}\right)\left(1 - \frac{1}{z_f}\right)\right], \tag{20}$$

where $\hat{x} = x_B/x$, α_s is the strong coupling constant, and e_c is the electric charge of the charm quark. We show all hard cross sections $\hat{\sigma}_i$ in the Appendix because they are lengthy. The result in the J/ψ rest frame is also available in [39].

B. Twist-3 polarized cross section for J/ψ production in SIDIS

We next calculate the twist-3 polarized cross section formula. The twist-3 quark distribution effect shown in Fig. 3 could also contribute to the SSA, and it was calculated in pp collision [40]. However, it is out of

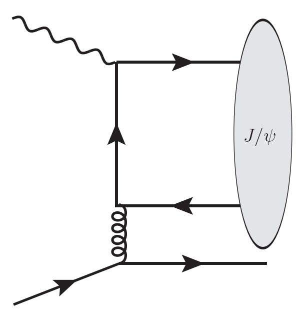

FIG. 3. A typical diagram given by the quark distribution effect. This is canceled in the color-singlet case in SIDIS.

scope of the present study because it vanishes in the color-singlet case in SIDIS. The general formula for the twist-3 gluon contribution in SIDIS was derived in [41] as

$$W_{\rho\sigma}^{\text{twist}-3}(p,q,P_{J/\psi}) = \langle \mathcal{O}^{J/\psi}({}^3S_1^{[1]})\rangle \Bigg\{ \omega_\alpha^\mu \omega_\beta^\nu \omega_\gamma^\lambda \int \frac{dx}{x^2} \Phi_\partial^{\alpha\beta\gamma}(x) \frac{\partial}{\partial k^\lambda} S_{\mu\nu,\rho\sigma}(k)|_{k=xp} \\ - \frac{1}{2}\omega_\alpha^\mu \omega_\beta^\nu \omega_\gamma^\lambda \int dx_1 \int dx_2 \left[\frac{-if^{abc}}{N_c(N_c^2-1)} N^{\alpha\beta\gamma}(x_1,x_2) + \frac{N_c d^{abc}}{(N_c^2-4)(N_c^2-1)} O^{\alpha\beta\gamma}(x_1,x_2) \right] \\ \times \frac{1}{x_1 - i\epsilon} \frac{1}{x_2 + i\epsilon} \frac{1}{x_2 - x_1 - i\epsilon} S^{abc}_{\mu\nu\lambda,\rho\sigma}(x_1 p, x_2 p) \Bigg\}, \tag{21}$$

where $\omega_\alpha^\mu = g_\alpha^\mu - p^\mu n_\alpha$. $S_{\mu\nu,\rho\sigma}(k)$ is given by

$$S_{\mu\nu,\rho\sigma}(k) = H_{\mu\nu,\rho\sigma}(k) 2\pi\delta[(k+q-P_{J/\psi})^2], \tag{22}$$

where the hard part $H_{\mu\nu,\rho\sigma}(k)$ is given by the diagrams in Fig. 2 by replacing the momentum xp with k. $S^{abc}_{\mu\nu\lambda,\rho\sigma}(x_1p, x_2p)$ can be separated into two parts as

$$S^{abc}_{\mu\nu\lambda,\rho\sigma}(x_1p,x_2p) = H^{abc}_{L\mu\nu\lambda,\rho\sigma}(x_1p,x_2p) 2\pi\delta[(x_2p+q-P_{J/\psi})^2] + H^{abc}_{R\mu\nu\lambda,\rho\sigma}(x_1p,x_2p) 2\pi\delta[(x_1p+q-P_{J/\psi})^2]. \tag{23}$$

$H^{abc}_{L\mu\nu\lambda,\rho\sigma}(x_1p,x_2p)$ is given by the product of the diagrams in Fig. 4 and the complex conjugate of the diagrams in Fig. 2. $H^{abc}_{R\mu\nu\lambda,\rho\sigma}(x_1p,x_2p)$ is the complex conjugate of $H^{abc}_{L\mu\nu\lambda,\rho\sigma}(x_1p,x_2p)$. From our direct calculation of the diagrams, we have observed that $H^{abc}_{L\mu\nu\lambda,\rho\sigma}(x_1p,x_2p)$ and $H^{abc}_{R\mu\nu\lambda,\rho\sigma}(x_1p,x_2p)$ have the following structures:

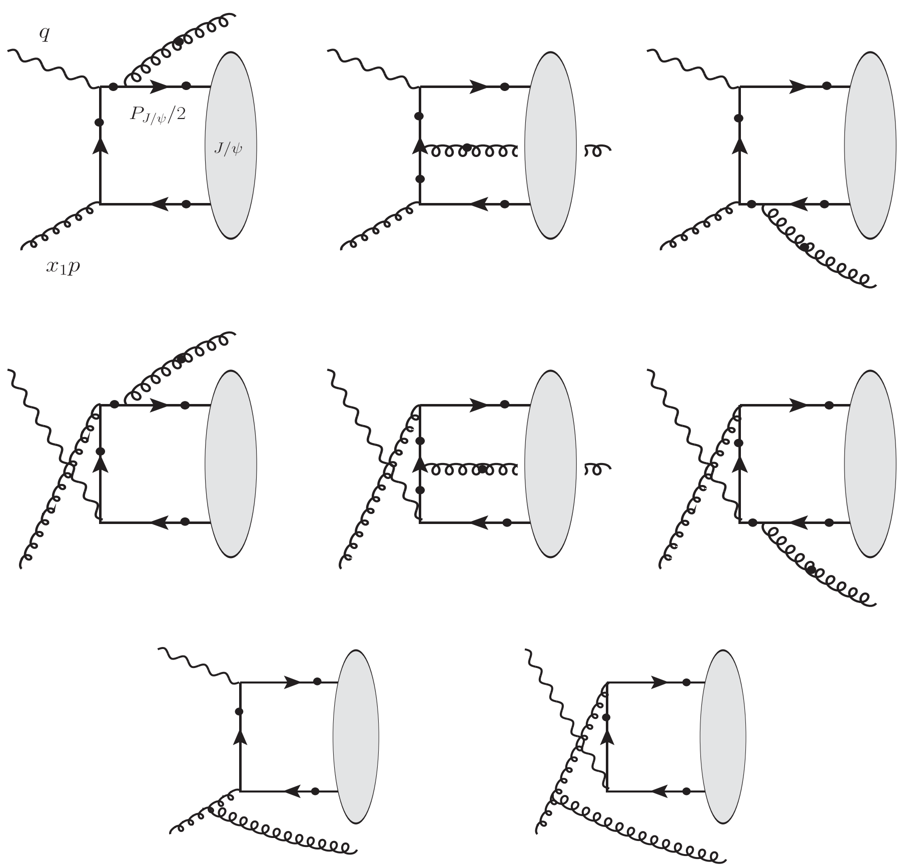

FIG. 4. Diagrams that contribute to $H^{abc}_{L\mu\nu\lambda,\rho\sigma}(x_1p,x_2p)$. The external gluon line with the momentum $(x_2-x_1)p$ is connected to one of the black dots. Thus, there are 36 diagrams in this figure. We ignored some diagrams that obviously vanish.

$$
\begin{aligned}
\frac{1}{x_1-i\epsilon}\frac{1}{x_2-x_1-i\epsilon}H^{abc}_{L\mu\nu\lambda,\rho\sigma}(x_1p,x_2p) &= \frac{1}{x_1-i\epsilon}H^{1\,abc}_{L\mu\nu\lambda,\rho\sigma}(x_2p)+\frac{x_2}{(x_1-i\epsilon)^2}H^{2\,abc}_{L\mu\nu\lambda,\rho\sigma}(x_2p)+\frac{1}{x_2-x_1-i\epsilon}H^{3\,abc}_{L\mu\nu\lambda,\rho\sigma}(x_2p)\\
&+\frac{x_2}{(x_2-x_1-i\epsilon)^2}H^{4\,abc}_{L\mu\nu\lambda,\rho\sigma}(x_2p)+\frac{1}{x_1-Ax+i\epsilon}H^{5\,abc}_{L\mu\nu\lambda,\rho\sigma}(x_2p)\\
&+\frac{1}{x_1-(1-A)x-i\epsilon}H^{6\,abc}_{L\mu\nu\lambda,\rho\sigma}(x_2p),\\
\frac{1}{x_2+i\epsilon}\frac{1}{x_2-x_1-i\epsilon}H^{abc}_{R\mu\nu\lambda,\rho\sigma}(x_1p,x_2p) &= \frac{1}{x_2+i\epsilon}H^{1\,abc}_{R\mu\nu\lambda,\rho\sigma}(x_1p)+\frac{x_1}{(x_2+i\epsilon)^2}H^{2\,abc}_{R\mu\nu\lambda,\rho\sigma}(x_1p)\\
&+\frac{1}{x_2-x_1-i\epsilon}H^{3\,abc}_{R\mu\nu\lambda,\rho\sigma}(x_1p)+\frac{x_1}{(x_2-x_1-i\epsilon)^2}H^{4\,abc}_{R\mu\nu\lambda,\rho\sigma}(x_1p)\\
&+\frac{1}{x_2-Ax-i\epsilon}H^{5\,abc}_{R\mu\nu\lambda,\rho\sigma}(x_1p)+\frac{1}{x_2-(1-A)x+i\epsilon}H^{6\,abc}_{R\mu\nu\lambda,\rho\sigma}(x_1p),
\end{aligned}
\tag{24}
$$

where $A=\frac{Q^2(1+\hat{x}-z_f)+m^2_{J/\psi}\hat{x}}{Q^2(2-z_f)}$. Substituting (1), (5), and (6) into $W^{\text{twist-3}}_{\rho\sigma}(p,q,P_{J/\psi})$, we can derive the following form:

$$
\begin{aligned}
W^{\text{twist-3}}_{\rho\sigma}(p,q,P_{J/\psi}) &= 2\pi\langle\mathcal{O}^{J/\psi}({}^3S_1^{[1]})\rangle\int\frac{dx}{x^2}\delta((xp+q-P_{J/\psi})^2)\bigg\{\left(x\frac{d}{dx}G_T^{(1)}(x)-2G_T^{(1)}(x)\right)H^{G1}_{\rho\sigma}+G_T^{(1)}(x)H^{G2}_{\rho\sigma}\\
&+\left(x\frac{d}{dx}\Delta H_T^{(1)}(x)-2\Delta H_T^{(1)}(x)\right)H^{H1}_{\rho\sigma}+\Delta H_T^{(1)}(x)H^{H2}_{\rho\sigma}\\
&+\int dx'\sum_i\bigg[\left(\frac{1}{x-x'-i\epsilon}H^{Ni}_{1L\rho\sigma}+\frac{x}{(x-x'-i\epsilon)^2}H^{Ni}_{2L\rho\sigma}+\frac{1}{x'-Ax+i\epsilon}H^{Ni}_{3L\rho\sigma}\right)N^i(x',x)\\
&+\left(\frac{1}{x-x'+i\epsilon}H^{Ni}_{1R\rho\sigma}+\frac{x}{(x-x'+i\epsilon)^2}H^{Ni}_{2R\rho\sigma}+\frac{1}{x'-Ax-i\epsilon}H^{Ni}_{3R\rho\sigma}\right)N^i(x,x')\\
&+\left(\frac{1}{x-x'-i\epsilon}H^{Oi}_{1L\rho\sigma}+\frac{x}{(x-x'-i\epsilon)^2}H^{Oi}_{2L\rho\sigma}+\frac{1}{x'-Ax+i\epsilon}H^{Oi}_{3L\rho\sigma}\right)O^i(x',x)\\
&+\left(\frac{1}{x-x'+i\epsilon}H^{Oi}_{1R\rho\sigma}+\frac{x}{(x-x'+i\epsilon)^2}H^{Oi}_{2R\rho\sigma}+\frac{1}{x'-Ax-i\epsilon}H^{Oi}_{3R\rho\sigma}\right)O^i(x,x')\bigg]\bigg\},
\end{aligned}
\tag{25}
$$

where we used the shorthand notations:

$$
\begin{aligned}
N^{1,2,3}(x',x) &= \{N(x',x),N(x,x-x'),N(x',x'-x)\},\\
O^{1,2,3}(x',x) &= \{O(x',x),O(x,x-x'),O(x',x'-x)\}.
\end{aligned}
\tag{26}
$$

We changed the integral variable as $x'\to x-x'$ for the denominators $1/(x'\pm i\epsilon)$ and $1/(x'-(1-A)x\pm i\epsilon)$ and used the symmetries (7). One can derive the cross section formula by taking a contraction with tensors $\tilde{\mathcal{V}}_i^{\rho\sigma}$. We have observed from our direct calculation that the contribution from the C-odd function $O(x_1,x_2)$ is exactly canceled. This can be naturally understood from the fact that the charm-anticharm pair is charge neutral. We can eliminate x'-integral by performing the following contour integrations:

$$
\begin{aligned}
\frac{1}{x'-x-i\epsilon}-\frac{1}{x'-x+i\epsilon} &= 2\pi i\delta(x'-x),\\
\frac{1}{x'-Ax-i\epsilon}-\frac{1}{x'-Ax+i\epsilon} &= 2\pi i\delta(x'-Ax),\\
\frac{1}{(x'-x+i\epsilon)^2}-\frac{1}{(x'-x-i\epsilon)^2} &= 2\pi i\frac{\partial}{\partial x'}\delta(x'-x).
\end{aligned}
\tag{27}
$$

The kinematical functions $G_T^{(1)}(x)$ and $\Delta H_T^{(1)}(x)$ can be eliminated by using the relations (8). As a result, we can write down the cross section formula only in terms of the C-even function $N(x_1,x_2)$ as

$$\frac{d^6\Delta\sigma}{dx_B dQ^2 dz_f dP_T^2 d\phi d\chi} = \frac{\alpha_{em}^2 \alpha_s^2 e_c^2 (2\pi M_N)}{4\pi S_{ep}^2 x_B^2 Q^2} \left(\mathcal{N}\langle \mathcal{O}^{J/\psi}({}^3S_1^{[1]})\rangle\right) \sum_{i=1,\ldots,4,8,9} \mathcal{A}_i(\phi-\chi)\mathcal{S}_i(\Phi_S-\chi)$$
$$\times \int \frac{dx}{x^2}\delta\left[\frac{P_T^2}{Q^2} - \left(1-\frac{1}{\hat{x}}+\frac{m_{J/\psi}^2}{z_f Q^2}\right)\left(1-\frac{1}{z_f}\right)\right]\left[N(x,x)\sigma_i^{N1} + N(x,0)\sigma_i^{N2} + N(x,Ax)\sigma_i^{N3}\right.$$
$$\left. + N(x,(1-A)x)\sigma_i^{N4} + N(Ax,-(1-A)x)\sigma_i^{N5}\right], \tag{28}$$

where $\mathcal{S}_i(\Phi_S-\chi) = \sin(\Phi_S-\chi)(i=1,2,3,4), \cos(\Phi_S-\chi)$ ($i=8$, 9). All hard cross sections are shown in the Appendix. It turns out that the derivative terms $\frac{d}{dx}N(x,x)$ and $\frac{d}{dx}N(x,0)$ given by (27) are exactly canceled in the color singlet channel, which is consistent with the statement made in [42]. However, we have observed that nonzero contributions from nonderivative terms $N(x,x)$ and $N(x,0)$ survive even in the color-singlet case. The hard cross sections (A6)–(A17) show that the most singular term with respect to small-P_T is $P_T/(1-z_f) \sim 1/P_T$ in the color-singlet contribution. This term is ignored in the context of the matching between the TMD, and the collinear frameworks as a relatively suppressed contribution in the small-P_T region, which is the reason why it was not important in the discussion in [42]. However, less singular terms with respect to small-P_T are relatively enhanced in high-P_T region and, therefore, there is no reason to ignore them. We will see in the next section that the contributions from $N(x,x)$ and $N(x,0)$ could be sizable at the EIC kinematics. In addition, there are other contributions $N(x,Ax)$, $N(x,(1-A)x)$, and $N(Ax,Ax-x)$ that can be regarded as the hard-pole contribution in the sense of the conventional pole calculation. A similar contribution was also observed in the case of the twist-3 quark distribution [40]. If the color-singlet contribution is dominant in J/ψ production, LDME is exactly canceled between the unpolarized cross section (20) and the polarized cross section (28) in the ratio. Thus, we can conclude that the SSA in the J/ψ production is an ideal observable to investigate the C-even twist-3 gluon distribution function $N(x_1,x_2)$ by eliminating other nonperturbative effects like the C-odd type twist-3 effect and the hadronization effect of J/ψ.

IV. NUMERICAL CALCULATION FOR THE SSA IN THE J/ψ PRODUCTION

We perform numerical simulations of the J/ψ SSA for the kinematics accessible at the future EIC experiment. The polarized cross section (28) can be expanded in terms of five structure functions $\mathcal{F}_i (i=1,2,\ldots 5)$ as

$$\frac{d^6\Delta\sigma}{dx_B dQ^2 dz_f dP_T^2 d\phi d\chi} = \sin(\phi_h-\phi_S)(\mathcal{F}_1 + \mathcal{F}_2\cos\phi_h + \mathcal{F}_3\cos 2\phi_h) + \cos(\phi_h-\phi_S) \times (\mathcal{F}_4\sin\phi_h + \mathcal{F}_5\sin 2\phi_h), \tag{29}$$

where the azimuthal dependences are defined by

$$\phi_h = \phi-\chi, \qquad \phi_h-\phi_S = \Phi_S-\chi. \tag{30}$$

The unpolarized cross section is given by

$$\frac{d^6\sigma}{dx_B dQ^2 dz_f dP_T^2 d\phi d\chi} = \sigma_1^{\rm U} + \sigma_2^{\rm U}\cos\phi_h + \sigma_3^{\rm U}\cos 2\phi_h. \tag{31}$$

We calculate five normalized structure functions [30],

$$\frac{\mathcal{F}_1}{\sigma_1^{\rm U}}, \quad \frac{\mathcal{F}_2}{2\sigma_1^{\rm U}}, \quad \frac{\mathcal{F}_3}{2\sigma_1^{\rm U}}, \quad \frac{\mathcal{F}_4}{2\sigma_1^{\rm U}}, \quad \frac{\mathcal{F}_5}{2\sigma_1^{\rm U}}. \tag{32}$$

We here show the explicit form of $\mathcal{F}_1/\sigma_1^{\rm U}$ that can be derived from (19), (20), and (28).

$$\frac{\mathcal{F}_1}{\sigma_1^{\rm U}} = \frac{2\pi M_N}{\left[\frac{4}{y^2}\left(1-y+\frac{y^2}{2}\right)\hat{\sigma}_1 - 2\hat{\sigma}_2\right]\bar{x}G(\bar{x})} \times \left[\frac{4}{y^2}\left(1-y+\frac{y^2}{2}\right)\left(\sum_{i=1}^{5} N^i(\bar{x})\sigma_1^{Ni}\right) - 2\left(\sum_{i=1}^{5} N^i(\bar{x})\sigma_2^{Ni}\right)\right], \tag{33}$$

where we defined

$$N^{1,2,3,4,5}(x) = \{N(x,x), N(x,0), N(x,Ax), N(x,(1-A)x), N(Ax,-(1-A)x)\}, \tag{34}$$

$$\bar{x} = x_B\left(1 + \frac{m_{J/\psi}^2}{z_f Q^2} + \frac{P_T^2}{Q^2}\frac{z_f}{1-z_f}\right). \tag{35}$$

One can easily derive other normalized structure functions in the same way. The LDME is exactly canceled as stated above and, therefore, the nonperturbative effect simply arises from ratios of twist-3 and twist-2 gluon distributions. The C-even function $N(x_1,x_2)$ has not been well constrained by experiment so far. We use the following simple models used in [29]:

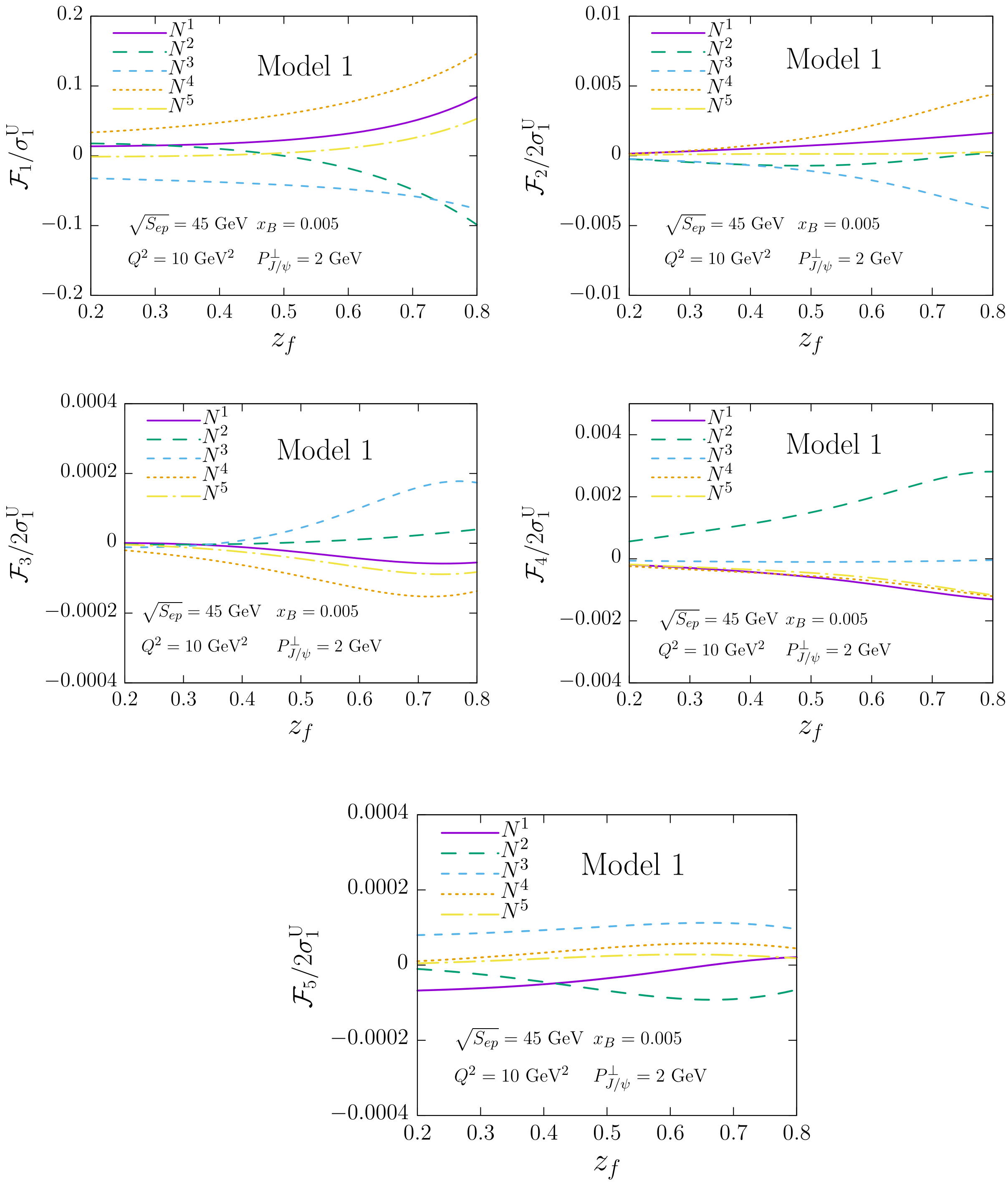

FIG. 5. Numerical calculations for the normalized structure functions in (32). $N^{1,2,3,4,5}$, respectively, show the contributions from the five functions $N(x,x)$, $N(x,0)$, $N(x,Ax)$, $N(x,(1-A)x)$, $N(Ax,-(1-A)x)$ with the model 1 function (36).

$$\text{model 1: } 0.002xG(x), \tag{36}$$

$$\text{model 2: } 0.0005\sqrt{x}G(x). \tag{37}$$

Experimental investigations of the twist-3 gluon contributions were reported in the past couple of years [43,44]. The magnitudes of the above models are consistent with the upper bound of the data. Each structure function depends on five types of C-even functions $\{N(x,x), N(x,0), N(x,Ax), N(x,(1-A)x), N(Ax,-(1-A)x)\}$. We separately plot the contributions from those five functions by substituting one of the models into each function.

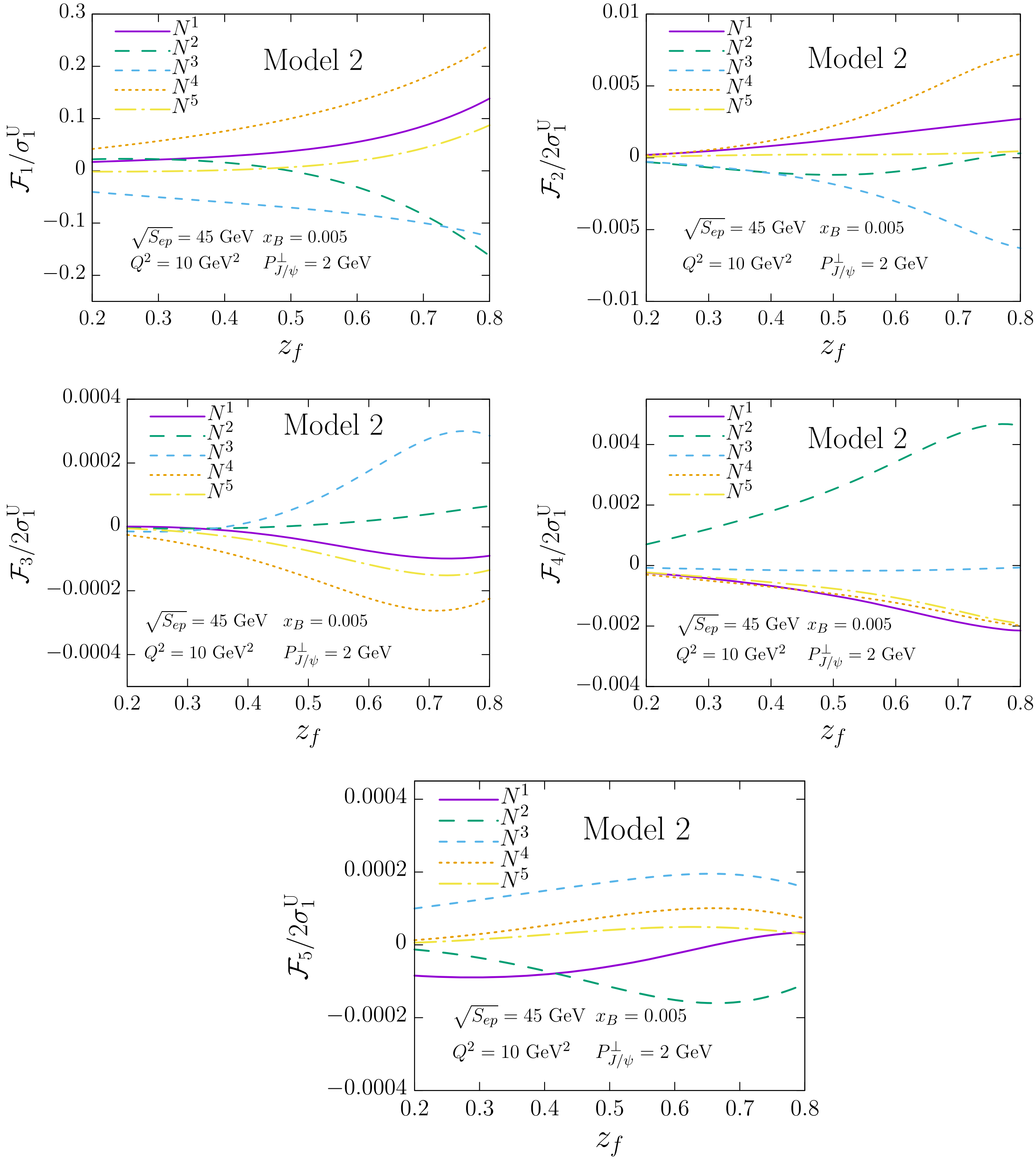

FIG. 6. Numerical calculations for the normalized structure functions with the model 2 function (37).

Models for $N(x, Ax)$, $N(x, (1-A)x)$, $N(Ax, -(1-A)x)$ should take the A dependence into account for realistic simulations. However, we use the above A-independent models for these functions because our current knowledge about the functions is very limited. Our simulations are still beneficial because they show some differences in the qualitative behavior among the hard cross sections. We perform our simulations with typical EIC kinematic valuables [3]: $\sqrt{S_{ep}} = 45$ GeV, $Q^2 = 10$ GeV^2, $x_B = 0.005$, $P_{J/\psi}^{\perp} = 2$ GeV. Figures 5 and 6, respectively, show our simulations with the models 1 and 2 for the five structure functions. The contributions from the five types of functions show different qualitative behaviors in each normalized structure function. These simulations could help to clarify which function is dominant in the J/ψ SSA by comparing with the data from EIC. Our simulations show that the difference in the x dependence between the models 1 and 2 does not cause a significant change in the qualitative behaviors. However, we find that the magnitudes of the contributions are uniformly increased in the model 2 compared to the model 1. This reflects the fact that the model 2 is more singular with respect to x and, therefore, it is enhanced at the small value of x_B. The observation of the enhancement could give us the information about the small-x behavior of the C-even function. The future EIC experiment plans to investigate the proton structure in a wide range of x_B, $10^{-3} \lesssim x_B \lesssim 0.5$. The measurement of J/ψ SSA at the EIC is a great opportunity to understand the small-x behavior of the higher twist gluon distribution function.

V. SUMMARY

We performed the first calculation for the twist-3 gluon contribution to the J/ψ SSA within the collinear framework. We observed that one of the possible twist-3 contributions, C-odd type twist-3 gluon contribution, is exactly canceled in the spin-dependent cross section formula. The cancellation partially happens to also the C-even type function. The derivative terms $\frac{d}{dx}N(x,x)$ and $\frac{d}{dx}N(x,0)$ are exactly canceled, while nonderivative terms $N(x,x)$ and $N(x,0)$ survive in the cross section. It was once stated that the soft-gluon-pole type contribution is exactly canceled in the color singlet contribution in SIDIS [42]. However, our result shows that this statement is not valid in high-P_T region where the relationship between the TMD and the collinear frameworks does not hold. In addition, we obtained the contributions from another type of the pole contributions whose existence was pointed out in [40] in the case of the twist-3 quark distribution. We have completed the LO cross section formula for the J/ψ SSA in the color-singlet case. Our result enables future investigations of the twist-3 gluon distribution function at the EIC. We performed some numerical simulations for the structure functions in the polarized cross section at the EIC kinematics. The qualitative differences among the five types of the C-even functions could help to pin down the dominant contribution to the J/ψ SSA. Our simulations show the correlation between the magnitudes of the structure functions and the x dependence of the twist-3 gluon distribution function. Future investigations in a wide range of the Bjorken variable at the EIC will provide rich information about the little-known twist-3 gluon distribution function.

ACKNOWLEDGMENTS

This work is supported by the National Natural Science Foundation of China under Grants No. 12022512 and No. 12035007, by the Guangdong Major Project of Basic and Applied Basic Research No. 2020B030103000, No. 2022A1515010683, and No. 2020A1515010794 and research startup funding at South China Normal University.

APPENDIX: LIST OF HARD CROSS SECTIONS

1. Hard cross sections of the unpolarized cross section in (20)

$$\hat{\sigma}_1 = \frac{1}{z_f^2[Q^2(-1+\hat{x})+m_{J/\psi}^2\hat{x}]^2[m_{J/\psi}^2\hat{x}+Q^2(1+\hat{x}-z_f)]^2} \times 64 m_{J/\psi}^2\hat{x}^2\Big(m_{J/\psi}^6\hat{x}^2(1-z_f+z_f^2)+m_{J/\psi}^2Q^4[1+(-2+4\hat{x}-7\hat{x}^2)z_f+(3-18\hat{x}+22\hat{x}^2)z_f^2 -2(1-8\hat{x}+9\hat{x}^2)z_f^3+(1-6\hat{x}+6\hat{x}^2)z_f^4]+Q^6(-1+\hat{x})z_f[-z_f+\hat{x}(-1+2z_f)]+m_{J/\psi}^4Q^2\hat{x}[z_f(-3+3z_f-2z_f^2) +\hat{x}(-5+17z_f-15z_f^2+6z_f^3)]\Big), \tag{A1}$$

$$\hat{\sigma}_2 = \frac{1}{z_f^2[Q^2(-1+\hat{x})+m_{J/\psi}^2\hat{x}]^2[m_{J/\psi}^2\hat{x}+Q^2(1+\hat{x}-z_f)]^2} \times 64 m_{J/\psi}^2Q^2\hat{x}^2\Big(Q^4(-1+\hat{x})^2z_f^2+2m_{J/\psi}^2Q^2(-1+\hat{x})\hat{x}z_f(-1+6z_f-6z_f^2+2z_f^3) + m_{J/\psi}^4\hat{x}^2(-2+10z_f-11z_f^2+4z_f^3)\Big), \tag{A2}$$

$$\hat{\sigma}_3 = \frac{1}{z_f[Q^2(-1+\hat{x}) + m_{J/\psi}^2\hat{x}]^2[m_{J/\psi}^2\hat{x} + Q^2(1+\hat{x}-z_f)]^2} \times 64 m_{J/\psi}^2 Q P_T \hat{x}^3 \Big(Q^4(-1+\hat{x})z_f + m_{J/\psi}^4\hat{x}(3-4z_f+2z_f^2) + m_{J/\psi}^2 Q^2[z_f(-3+4z_f-2z_f^2) + \hat{x}(-1+9z_f-10z_f^2+4z_f^3)]\Big), \tag{A3}$$

$$\hat{\sigma}_4 = -\frac{64 m_{J/\psi}^4 \hat{x}^3(-1+z_f)[m_{J/\psi}^2\hat{x} + Q^2(-1+\hat{x})z_f][m_{J/\psi}^2 + Q^2(-1+4z_f-2z_f^2)]}{z_f^2[Q^2(-1+\hat{x}) + m_{J/\psi}^2\hat{x}]^2[m_{J/\psi}^2\hat{x} + Q^2(1+\hat{x}-z_f)]^2}, \tag{A4}$$

$$\hat{\sigma}_8 = \hat{\sigma}_9 = 0. \tag{A5}$$

2. Hard cross sections of $N(x,x)$ in (28)

$$\begin{aligned}
\hat{\sigma}_1^{N1} = {} & \frac{-1}{(1-z_f)z_f^2 Q^2[Q^2(-1+\hat{x}) + m_{J/\psi}^2\hat{x}]^3[m_{J/\psi}^2\hat{x} + Q^2(1+\hat{x}-z_f)]^3} \\
& \times 128 m_{J/\psi}^2 P_T \hat{x}^3 \Big(2m_{J/\psi}^{10}\hat{x}^4(5-6z_f+3z_f^2) + 4Q^{10}(-1+\hat{x})z_f[1-5z_f+3z_f^2-z_f^3 \\
& + \hat{x}^3(-1+2z_f) + \hat{x}^2(z_f-4z_f^2) + \hat{x}(-2+7z_f-3z_f^2+2z_f^3)] \\
& + 2m_{J/\psi}^8 Q^2\hat{x}^3[-2z_f(8-9z_f+5z_f^2) + \hat{x}(-9+58z_f-65z_f^2+26z_f^3)] \\
& + m_{J/\psi}^6 Q^4\hat{x}^2[18-34z_f+77z_f^2-63z_f^3+30z_f^4-16\hat{x}z_f(-3+19z_f-20z_f^2+8z_f^3) \\
& + 2\hat{x}^2(-33+112z_f-65z_f^2-18z_f^3+24z_f^4)] + m_{J/\psi}^4 Q^6\hat{x}[z_f(-54+106z_f-123z_f^2+71z_f^3-24z_f^4) \\
& - 4\hat{x}^2 z_f(-25+84z_f-27z_f^2-32z_f^3+24z_f^4) + 2\hat{x}^3(-19+24z_f+81z_f^2-114z_f^3+48z_f^4) \\
& + 2\hat{x}(-9+65z_f-123z_f^2+224z_f^3-177z_f^4+62z_f^5)] + m_{J/\psi}^2 Q^8[4-12z_f+47z_f^2-74z_f^3+67z_f^4-32z_f^5+8z_f^6 \\
& + 4\hat{x}^4 z_f(-13+41z_f-35z_f^2+12z_f^3) - 8\hat{x}^3 z_f(-3+31z_f^2-32z_f^3+12z_f^4) \\
& + \hat{x}z_f(28-220z_f+363z_f^2-359z_f^3+188z_f^4-48z_f^5) \\
& + \hat{x}^2(12-84z_f+229z_f^2-157z_f^3+152z_f^4-116z_f^5+48z_f^6)]\Big),
\end{aligned} \tag{A6}$$

$$\begin{aligned}
\hat{\sigma}_2^{N1} = {} & \frac{-1}{(1-z_f)z_f^2[Q^2(-1+\hat{x}) + m_{J/\psi}^2\hat{x}]^3[m_{J/\psi}^2\hat{x} + Q^2(1+\hat{x}-z_f)]^3} \\
& \times 512 m_{J/\psi}^2 P_T \hat{x}^3 \Big(Q^8(-1+\hat{x})^2 z_f^2(3+\hat{x}^2-2z_f-2\hat{x}z_f+z_f^2) + m_{J/\psi}^8\hat{x}^4(-4+20z_f-23z_f^2+8z_f^3) \\
& + 2m_{J/\psi}^6 Q^2\hat{x}^3[z_f(5-26z_f+29z_f^2-10z_f^3) + 2\hat{x}(-2+9z_f-6z_f^2-2z_f^3+2z_f^4)] \\
& + m_{J/\psi}^4 Q^4\hat{x}^2[-4+24z_f-50z_f^2+84z_f^3-67z_f^4+20z_f^5+2\hat{x}z_f(6-29z_f+13z_f^2+12z_f^3-8z_f^4) \\
& + 2\hat{x}^2(-2+6z_f+11z_f^2-20z_f^3+8z_f^4)] + 2m_{J/\psi}^2 Q^6\hat{x}z_f[3-21z_f+36z_f^2-35z_f^3+18z_f^4-4z_f^5 \\
& + 2\hat{x}^3(-1+6z_f-6z_f^2+2z_f^3) + \hat{x}^2(1-4z_f-17z_f^2+22z_f^3-8z_f^4) + \hat{x}(-2+13z_f-7z_f^2+9z_f^3-10z_f^4+4z_f^5)]\Big),
\end{aligned} \tag{A7}$$

$$\begin{aligned}\hat{\sigma}_3^{N1} = {}& \frac{1}{z_f^3 Q[Q^2(-1+\hat{x}) + m_{J/\psi}^2\hat{x}]^3[m_{J/\psi}^2\hat{x} + Q^2(1+\hat{x}-z_f)]^3} \\ & \times 128 m_{J/\psi}^2 \hat{x}^2 \Big(2m_{J/\psi}^{10}\hat{x}^5(13-21z_f+10z_f^2) + Q^{10}(-1+\hat{x})^2 z_f^2[4\hat{x}^3 + 3(-1+z_f) - 8\hat{x}^2 z_f + \hat{x}(9-8z_f+4z_f^2)] \\ & + m_{J/\psi}^8 Q^2\hat{x}^4[z_f(-83+129z_f-62z_f^2) + \hat{x}(46-78z_f^2+52z_f^3)] \\ & + m_{J/\psi}^6 Q^4\hat{x}^3[22-48z_f+148z_f^2-177z_f^3+80z_f^4-\hat{x}z_f(101+53z_f-226z_f^2+136z_f^3) \\ & + 2\hat{x}^2(7+62z_f-79z_f^2+14z_f^3+16z_f^4)] + m_{J/\psi}^2 Q^8\hat{x}z_f[4+35z_f-92z_f^2+100z_f^3-58z_f^4+16z_f^5 \\ & + \hat{x}^4(-2+66z_f-76z_f^2+32z_f^3) + \hat{x}^3(1-71z_f-50z_f^2+120z_f^3-64z_f^4) \\ & + \hat{x}^2(-2+94z_f-15z_f^2-6z_f^3-28z_f^4+32z_f^5) - \hat{x}(1+124z_f-233z_f^2+246z_f^3-150z_f^4+48z_f^5)] \\ & + m_{J/\psi}^4 Q^6\hat{x}^2[z_f(-63+143z_f-192z_f^2+148z_f^3-54z_f^4) + 2\hat{x}^3(-3+40z_f+z_f^2-50z_f^3+32z_f^4) \\ & - \hat{x}^2 z_f(17+245z_f-246z_f^2+16z_f^3+64z_f^4) + \hat{x}(-10+110z_f-123z_f^2+248z_f^3-282z_f^4+132z_f^5)]\Big), \end{aligned} \tag{A8}$$

$$\begin{aligned}\hat{\sigma}_4^{N1} = {}& \frac{1}{z_f^2 Q^2[Q^2(-1+\hat{x}) + m_{J/\psi}^2\hat{x}]^3[m_{J/\psi}^2\hat{x} + Q^2(1+\hat{x}-z_f)]^3} \\ & \times 128 m_{J/\psi}^4 P_T \hat{x}^3 \Big(2m_{J/\psi}^8\hat{x}^4(-5+3z_f) + 2m_{J/\psi}^6 Q^2\hat{x}^3[-6(-2+z_f)z_f + \hat{x}(-7-11z_f+10z_f^2)] \\ & + m_{J/\psi}^4 Q^4\hat{x}^2[-6-13z_f^2+6z_f^3+12\hat{x}z_f(1+6z_f-4z_f^2) + 2\hat{x}^2(1-27z_f+6z_f^2+8z_f^3)] \\ & + Q^8(-1+\hat{x})z_f[-3(-1+z_f)z_f + 4\hat{x}^3(2-7z_f+4z_f^2) - 4\hat{x}^2(-1+7z_f-16z_f^2+8z_f^3) \\ & + \hat{x}(12-57z_f+76z_f^2-52z_f^3+16z_f^4)] + m_{J/\psi}^2 Q^6\hat{x}[-z_f(-10+4z_f+z_f^2) - 4\hat{x}^2 z_f(4-21z_f+8z_f^3) \\ & + 2\hat{x}^3(3-9z_f-18z_f^2+16z_f^3) + 2\hat{x}(5-28z_f+35z_f^2-47z_f^3+22z_f^4)]\Big), \end{aligned} \tag{A9}$$

$$\begin{aligned}\hat{\sigma}_8^{N1} = {}& \frac{1}{z_f^3 Q[Q^2(-1+\hat{x}) + m_{J/\psi}^2\hat{x}]^2[m_{J/\psi}^2\hat{x} + Q^2(1+\hat{x}-z_f)]^2} \\ & \times 128 m_{J/\psi}^2 \hat{x}^2 \Big(-Q^6(-1+\hat{x})z_f^2 + 2m_{J/\psi}^6\hat{x}^3(1-3z_f+2z_f^2) \\ & + m_{J/\psi}^4 Q^2\hat{x}^2(1-3z_f+2z_f^2)[-3z_f+2\hat{x}(1+z_f)] + m_{J/\psi}^2 Q^4\hat{x}z_f[z_f(-1-2z_f+2z_f^2) \\ & + \hat{x}^2(2-6z_f+4z_f^2) + \hat{x}(-1+z_f+4z_f^2-4z_f^3)]\Big), \end{aligned} \tag{A10}$$

$$\begin{aligned}\hat{\sigma}_9^{N1} = {}& \frac{128 m_{J/\psi}^4 P_T \hat{x}^3}{z_f^2 Q^2[Q^2(-1+\hat{x}) + m_{J/\psi}^2\hat{x}]^2[m_{J/\psi}^2\hat{x} + Q^2(1+\hat{x}-z_f)]^2}\Big(2m_{J/\psi}^4\hat{x}^2(-1+z_f) \\ & + 2m_{J/\psi}^2 Q^2\hat{x}(-1+z_f)(\hat{x}-z_f+2\hat{x}z_f) + Q^4 z_f[4\hat{x}^2(-1+z_f) + z_f - 4\hat{x}(-1+z_f)z_f]\Big). \end{aligned} \tag{A11}$$

3. Hard cross sections of $N(x,0)$ in (28)

$$\hat{\sigma}_1^{N2} = \frac{1}{(1-z_f)z_f^2Q^2[Q^2(-1+\hat{x})+m_{J/\psi}^2\hat{x}]^3[m_{J/\psi}^2\hat{x}+Q^2(1+\hat{x}-z_f)]^3} \times 128m_{J/\psi}^2P_T\hat{x}^3\Big(2m_{J/\psi}^{10}\hat{x}^4(9-10z_f+7z_f^2) + 4Q^{10}(-1+\hat{x})z_f[3-13z_f+13z_f^2-5z_f^3+\hat{x}^3(-3+6z_f)+\hat{x}^2(-2+9z_f-12z_f^2)+\hat{x}z_f(3-5z_f+6z_f^2)] + 2m_{J/\psi}^8Q^2\hat{x}^3[-2z_f(13-14z_f+9z_f^2)+\hat{x}(-21+118z_f-117z_f^2+50z_f^3)] + m_{J/\psi}^6Q^4\hat{x}^2[42-90z_f+131z_f^2-89z_f^3+42z_f^4-4\hat{x}z_f(-27+143z_f-142z_f^2+58z_f^3) + 6\hat{x}^2(-23+72z_f-31z_f^2-14z_f^3+16z_f^4)] + m_{J/\psi}^4Q^6\hat{x}[z_f(-94+206z_f-209z_f^2+105z_f^3-32z_f^4)-4\hat{x}^2z_f(-46+133z_f-11z_f^2-76z_f^3+48z_f^4) + 2\hat{x}^3(-39+32z_f+205z_f^2-234z_f^3+96z_f^4)+2\hat{x}(-17+145z_f-345z_f^2+514z_f^3-361z_f^4+118z_f^5)] + m_{J/\psi}^2Q^8[-4+12z_f+37z_f^2-106z_f^3+109z_f^4-52z_f^5+12z_f^6+4\hat{x}^4z_f(-31+93z_f-71z_f^2+24z_f^3) - 4\hat{x}^3z_f(-7-27z_f+152z_f^2-134z_f^3+48z_f^4)+\hat{x}z_f(96-572z_f+1041z_f^2-969z_f^3+460z_f^4-104z_f^5) + \hat{x}^2(20-92z_f+211z_f^2-199z_f^3+316z_f^4-244z_f^5+96z_f^6)]\Big), \tag{A12}$$

$$\hat{\sigma}_2^{N2} = \frac{1}{(1-z_f)z_f^2[Q^2(-1+\hat{x})+m_{J/\psi}^2\hat{x}]^3[m_{J/\psi}^2\hat{x}+Q^2(1+\hat{x}-z_f)]^3} \times 512m_{J/\psi}^2P_T\hat{x}^3\Big(Q^8(-1+\hat{x})^2z_f^2(5+3\hat{x}^2+\hat{x}(4-6z_f)-6z_f+3z_f^2)+m_{J/\psi}^8\hat{x}^4(-8+40z_f-45z_f^2+16z_f^3) + 2m_{J/\psi}^6Q^2\hat{x}^3[z_f(9-46z_f+51z_f^2-18z_f^3)+\hat{x}(-8+36z_f-22z_f^2-8z_f^3+8z_f^4)] + m_{J/\psi}^4Q^4\hat{x}^2[-8+48z_f-106z_f^2+160z_f^3-121z_f^4+36z_f^5+2\hat{x}z_f(10-45z_f+11z_f^2+28z_f^3-16z_f^4) + \hat{x}^2(-8+24z_f+50z_f^2-80z_f^3+32z_f^4)]+2m_{J/\psi}^2Q^6\hat{x}z_f[7-45z_f+84z_f^2-79z_f^3+38z_f^4-8z_f^5 + \hat{x}^3(-4+26z_f-24z_f^2+8z_f^3)+\hat{x}^2(1-43z_f^2+46z_f^3-16z_f^4)+\hat{x}(-4+19z_f-17z_f^2+25z_f^3-22z_f^4+8z_f^5)]\Big), \tag{A13}$$

$$\hat{\sigma}_3^{N2} = \frac{-1}{z_f^3Q(Q^2(-1+\hat{x})+m_{J/\psi}^2\hat{x})^3(m_{J/\psi}^2\hat{x}+Q^2(1+\hat{x}-z_f))^3} \times 128m_{J/\psi}^2\hat{x}^2\Big(2m_{J/\psi}^{10}\hat{x}^5(25-37z_f+18z_f^2)+Q^{10}(-1+\hat{x})^2z_f^2[-9+12\hat{x}^3+\hat{x}^2(10-24z_f)+15z_f-6z_f^2 + \hat{x}(5-12z_f+12z_f^2)]+m_{J/\psi}^8Q^2\hat{x}^4[z_f(-149+217z_f-106z_f^2)+2\hat{x}(43+16z_f-79z_f^2+50z_f^3)] + m_{J/\psi}^6Q^4\hat{x}^3[54-160z_f+346z_f^2-339z_f^3+144z_f^4-\hat{x}z_f(163+187z_f-454z_f^2+256z_f^3) + \hat{x}^2(22+284z_f-294z_f^2+44z_f^3+64z_f^4)]+m_{J/\psi}^2Q^8\hat{x}z_f[12+75z_f-268z_f^2+312z_f^3-166z_f^4+40z_f^5 + 2\hat{x}^4(-1+77z_f-78z_f^2+32z_f^3)+\hat{x}^3(7-137z_f-150z_f^2+256z_f^3-128z_f^4) + \hat{x}(1-184z_f+487z_f^2-602z_f^3+354z_f^4-104z_f^5)+\hat{x}^2(-18+92z_f+87z_f^2-30z_f^3-60z_f^4+64z_f^5)] + m_{J/\psi}^4Q^6\hat{x}^2[z_f(-153+443z_f-562z_f^2+362z_f^3-114z_f^4)+2\hat{x}^3(-7+88z_f+21z_f^2-106z_f^3+64z_f^4) - \hat{x}^2z_f(7+527z_f-434z_f^2+128z_f^4)+\hat{x}(-10+142z_f-263z_f^2+608z_f^3-602z_f^4+260z_f^5)]\Big), \tag{A14}$$

$$\hat{\sigma}_4^{N2} = \frac{-1}{z_f^2 Q^2 [Q^2(-1+\hat{x}) + m_{J/\psi}^2 \hat{x}]^3 [m_{J/\psi}^2 \hat{x} + Q^2(1+\hat{x}-z_f)]^3}$$
$$\times 128 m_{J/\psi}^4 P_T \hat{x}^3 \Big(6 m_{J/\psi}^8 \hat{x}^4(-3+z_f) + 2 m_{J/\psi}^6 Q^2 \hat{x}^3 [2(11-3z_f)z_f + \hat{x}(-11-31z_f+18z_f^2)]$$
$$+ m_{J/\psi}^4 Q^4 \hat{x}^2 [-22+40z_f-67z_f^2+18z_f^3+8\hat{x}z_f(2+21z_f-11z_f^2)+2\hat{x}^2(5-63z_f+6z_f^2+16z_f^3)]$$
$$+ Q^8 z_f [4\hat{x}^4(4-15z_f+8z_f^2)+3z_f(-11+23z_f-16z_f^2+4z_f^3)-8\hat{x}^3(1-13z_f^2+8z_f^3)$$
$$+\hat{x}(-8+88z_f-153z_f^2+124z_f^3-40z_f^4)+\hat{x}^2(16-43z_f-36z_f^3+32z_f^4)]$$
$$+ m_{J/\psi}^2 Q^6 \hat{x}[z_f(58-112z_f+89z_f^2-24z_f^3)-4\hat{x}^2 z_f(9-45z_f-4z_f^2+16z_f^3)$$
$$+2\hat{x}^3(7-21z_f-42z_f^2+32z_f^3)+2\hat{x}(5-36z_f+57z_f^2-103z_f^3+46z_f^4)]\Big), \tag{A15}$$

$$\hat{\sigma}_8^{N2} = \frac{-1}{z_f^3 Q [Q^2(-1+\hat{x}) + m_{J/\psi}^2 \hat{x}]^3 [m_{J/\psi}^2 \hat{x} + Q^2(1+\hat{x}-z_f)]^3}$$
$$\times 128 m_{J/\psi}^2 \hat{x}^2 \Big(-Q^{10}(-1+\hat{x})^2 z_f^2 (3+2\hat{x}^2+\hat{x}(5-4z_f)-5z_f+2z_f^2) + 2 m_{J/\psi}^{10} \hat{x}^5 (1-3z_f+2z_f^2)$$
$$+ m_{J/\psi}^6 Q^4 \hat{x}^3 [6-24z_f+50z_f^2-53z_f^3+24z_f^4+\hat{x}z_f(-21+27z_f+2z_f^2-16z_f^3)$$
$$+6\hat{x}^2(1-2z_f-z_f^2+2z_f^3)] + m_{J/\psi}^8 Q^2 \hat{x}^4 [z_f(-11+23z_f-14z_f^2)+2\hat{x}(3-8z_f+3z_f^2+2z_f^3)]$$
$$+ m_{J/\psi}^2 Q^8 \hat{x} z_f [\hat{x}^4(2-6z_f+4z_f^2)+\hat{x}^3(1-23z_f+30z_f^2-16z_f^3)$$
$$+z_f(17-56z_f+64z_f^2-34z_f^3+8z_f^4)+\hat{x}^2(6-24z_f+53z_f^2-46z_f^3+20z_f^4)$$
$$-\hat{x}(9-36z_f+31z_f^2+2z_f^3-14z_f^4+8z_f^5)] + m_{J/\psi}^4 Q^6 \hat{x}^2 [2\hat{x}^3(1-7z_f^2+6z_f^3)-\hat{x}^2 z_f(9+17z_f-46z_f^2+32z_f^3)$$
$$+z_f(-19+73z_f-102z_f^2+70z_f^3-22z_f^4)+\hat{x}(6-18z_f+27z_f^2-4z_f^3-22z_f^4+20z_f^5)]\Big), \tag{A16}$$

$$\hat{\sigma}_9^{N2} = \frac{-1}{z_f^2 Q^2 [Q^2(-1+\hat{x}) + m_{J/\psi}^2 \hat{x}]^3 [m_{J/\psi}^2 \hat{x} + Q^2(1+\hat{x}-z_f)]^3}$$
$$\times 128 m_{J/\psi}^4 P_T \hat{x}^3 \Big(2 m_{J/\psi}^8 \hat{x}^4(-1+z_f) + 2 m_{J/\psi}^6 Q^2 \hat{x}^3[-2(-2+z_f)z_f+\hat{x}(-3+z_f+2z_f^2)]$$
$$+ m_{J/\psi}^4 Q^4 \hat{x}^2[-6+12z_f-17z_f^2+6z_f^3+6\hat{x}^2(-1-z_f+2z_f^2)-4\hat{x}z_f(-3-4z_f+4z_f^2)]$$
$$+ Q^8 z_f[4\hat{x}^4(-1+z_f)-4\hat{x}^3(1-6z_f+4z_f^2)+z_f(-11+23z_f-16z_f^2+4z_f^3)$$
$$+\hat{x}^2(-12+31z_f-44z_f^2+20z_f^3)+\hat{x}(4-15z_f^2+20z_f^3-8z_f^4)]$$
$$+ m_{J/\psi}^2 Q^6 \hat{x}[4\hat{x}^2(11-8z_f)z_f^2+2\hat{x}^3(-1-5z_f+6z_f^2)+z_f(14-32z_f+27z_f^2-8z_f^3)$$
$$+2\hat{x}(-3+7z_f^2-19z_f^3+10z_f^4)]\Big). \tag{A17}$$

4. Hard cross sections of $N(x, Ax)$ in (28)

$$\sigma_1^{N3} = \frac{-1}{(1-z_f) z_f^2 [Q^2(-1+\hat{x}) + \hat{x} m_{J/\psi}^2]^3 [Q^2(1+\hat{x}-z_f) + \hat{x} m_{J/\psi}^2]^3}$$
$$\times 128 Q^2 P_T \hat{x}^3 m_{J/\psi}^2 \Big(4Q^6(-1+\hat{x})(-2+z_f)z_f[-z_f+\hat{x}(-1+2z_f)]$$
$$+ m_{J/\psi}^2 Q^4[-8+25z_f-50z_f^2+53z_f^3-32z_f^4+8z_f^5+\hat{x}^2(-4+103z_f-365z_f^2+446z_f^3-240z_f^4+48z_f^5)$$
$$-\hat{x}(4+48z_f-275z_f^2+383z_f^3-224z_f^4+48z_f^5)]$$
$$+ Q^2 m_{J/\psi}^4 \hat{x}[-2+50z_f-83z_f^2+59z_f^3-16z_f^4+\hat{x}(70-300z_f+396z_f^2-226z_f^3+48z_f^4)]$$
$$+ m_{J/\psi}^6 \hat{x}^2(-22+37z_f-27z_f^2+8z_f^3)\Big), \tag{A18}$$

$$\sigma_2^{N3} = \frac{-1}{(1-z_f)z_f^2[Q^2(-1+\hat{x})+\hat{x}m_{J/\psi}^2]^3[Q^2(1+\hat{x}-z_f)+\hat{x}m_{J/\psi}^2]^3} \times 512Q^4P_T\hat{x}^3(-2+z_f)m_{J/\psi}^2\Big(Q^4(-1+\hat{x})^2z_f^2+2m_{J/\psi}^2Q^2(-1+\hat{x})\hat{x}z_f(-2+11z_f-12z_f^2+4z_f^3) + m_{J/\psi}^4\hat{x}^2(-4+20z_f-23z_f^2+8z_f^3)\Big), \tag{A19}$$

$$\sigma_3^{N3} = \frac{1}{z_f^3[Q^2(-1+\hat{x})+\hat{x}m_{J/\psi}^2]^3[Q^2(1+\hat{x}-z_f)+\hat{x}m_{J/\psi}^2]^3} \times 256Q^3\hat{x}^3m_{J/\psi}^2\Big(2Q^6(-1+\hat{x})^2(-2+z_f)z_f^2+m_{J/\psi}^2Q^4z_f[-1-18z_f+41z_f^2-32z_f^3+8z_f^4 - 2\hat{x}(1-41z_f+76z_f^2-52z_f^3+12z_f^4)+\hat{x}^2(3-64z_f+111z_f^2-72z_f^3+16z_f^4)] + m_{J/\psi}^4Q^2\hat{x}[1+43z_f-91z_f^2+67z_f^3-16z_f^4+\hat{x}(7-91z_f+161z_f^2-107z_f^3+24z_f^4)] + m_{J/\psi}^6\hat{x}^2(-25+50z_f-35z_f^2+8z_f^3)\Big), \tag{A20}$$

$$\sigma_4^{N3} = \frac{1}{z_f^2[Q^2(-1+\hat{x})+\hat{x}m_{J/\psi}^2]^3[Q^2(1+\hat{x}-z_f)+\hat{x}m_{J/\psi}^2]^3} \times 128Q^2P_T\hat{x}^3m_{J/\psi}^4\Big(Q^4z_f[3-3z_f+\hat{x}(12-67z_f+64z_f^2-16z_f^3)+\hat{x}^2(-15+70z_f-64z_f^2+16z_f^3)] + m_{J/\psi}^2Q^2\hat{x}[-2-16z_f+11z_f^2+2\hat{x}(-7+43z_f-37z_f^2+8z_f^3)]+m_{J/\psi}^4\hat{x}^2(18-11z_f)\Big), \tag{A21}$$

$$\sigma_8^{N3} = -\frac{256Q^3\hat{x}^3(1-z_f)^2m_{J/\psi}^4[Q^2(-1+\hat{x})z_f+\hat{x}m_{J/\psi}^2]}{z_f^3[Q^2(-1+\hat{x})+\hat{x}m_{J/\psi}^2]^2[Q^2(1+\hat{x}-z_f)+\hat{x}m_{J/\psi}^2]^3}, \tag{A22}$$

$$\sigma_9^{N3} = -\frac{128Q^2P_T\hat{x}^3m_{J/\psi}^4(Q^2z_f[1-z_f+\hat{x}(-3+2z_f)]+m_{J/\psi}^2\hat{x}(-2+z_f))}{z_f^2[Q^2(-1+\hat{x})+\hat{x}m_{J/\psi}^2]^2[Q^2(1+\hat{x}-z_f)+\hat{x}m_{J/\psi}^2]^3}. \tag{A23}$$

5. Hard cross sections of $N(x,(1-A)x)$ in (28)

$$\sigma_1^{N4} = \frac{1}{(1-z_f)z_f^2[Q^2(-1+\hat{x})+\hat{x}m_{J/\psi}^2]^3[Q^2(1+\hat{x}-z_f)+\hat{x}m_{J/\psi}^2]^3} \times 128Q^2P_T\hat{x}^3m_{J/\psi}^2\Big(4Q^6(-1+\hat{x})z_f[-1+6z_f-3z_f^2+\hat{x}(3-9z_f+4z_f^2)]+m_{J/\psi}^2Q^4[-8+15z_f-34z_f^2+37z_f^3 - 24z_f^4+6z_f^5+\hat{x}(4-80z_f+361z_f^2-449z_f^3+248z_f^4-52z_f^5) + \hat{x}^2(-4+101z_f-379z_f^2+446z_f^3-236z_f^4+48z_f^5)] + m_{J/\psi}^4Q^2\hat{x}[2+46z_f-69z_f^2+49z_f^3-12z_f^4+\hat{x}(70-310z_f+400z_f^2-236z_f^3+52z_f^4)] + m_{J/\psi}^6\hat{x}^2(-22+33z_f-25z_f^2+6z_f^3)\Big), \tag{A24}$$

$$\sigma_2^{N4} = \frac{1}{(1-z_f)z_f^2[Q^2(-1+\hat{x})+\hat{x}m_{J/\psi}^2]^3[Q^2(1+\hat{x}-z_f)+\hat{x}m_{J/\psi}^2]^3} \times 1024Q^4P_T\hat{x}^3(-2+z_f)m_{J/\psi}^2\Big(Q^4(-1+\hat{x})^2z_f^2+2m_{J/\psi}^2Q^2(-1+\hat{x})\hat{x}z_f(-1+6z_f-6z_f^2+2z_f^3) + m_{J/\psi}^4\hat{x}^2(-2+10z_f-11z_f^2+4z_f^3)\Big), \tag{A25}$$

$$\sigma_3^{N4} = \frac{-1}{z_f^3[Q^2(-1+\hat{x})+\hat{x}m_{J/\psi}^2]^3[Q^2(1+\hat{x}-z_f)+\hat{x}m_{J/\psi}^2]^3} \times 128Q^3\hat{x}^2m_{J/\psi}^2\Big(Q^6(-1+\hat{x})^2z_f^2[3-3z_f+\hat{x}(-13+8z_f)]+m_{J/\psi}^2Q^4\hat{x}z_f[-2-55z_f+112z_f^2-80z_f^3+20z_f^4 - 4\hat{x}z_f(-46+83z_f-55z_f^2+13z_f^3)+\hat{x}^2(2-129z_f+220z_f^2-140z_f^3+32z_f^4)] + m_{J/\psi}^4Q^2\hat{x}^2[-2+110z_f-215z_f^2+157z_f^3-40z_f^4+\hat{x}(14-184z_f+319z_f^2-216z_f^3+52z_f^4)] + m_{J/\psi}^6\hat{x}^3(-50+102z_f-77z_f^2+20z_f^3)\Big), \tag{A26}$$

$$\sigma_4^{N4} = \frac{-1}{z_f^2(Q^2(-1+\hat{x})+\hat{x}m_{J/\psi}^2)^3(Q^2(1+\hat{x}-z_f)+\hat{x}m_{J/\psi}^2)^3} \times 128Q^2P_T\hat{x}^3m_{J/\psi}^4\Big(Q^4z_f[\hat{x}(12-65z_f+68z_f^2-20z_f^3) + 3(-1+5z_f-6z_f^2+2z_f^3)+\hat{x}^2(-17+66z_f-60z_f^2+16z_f^3)] + m_{J/\psi}^2Q^2\hat{x}[2-32z_f+37z_f^2-12z_f^3+2\hat{x}(-7+38z_f-36z_f^2+10z_f^3)]+m_{J/\psi}^4\hat{x}^2(18-19z_f+6z_f^2)\Big), \tag{A27}$$

$$\sigma_8^{N4} = \frac{-1}{z_f^3(Q^2(-1+\hat{x})+\hat{x}m_{J/\psi}^2)^3(Q^2(1+\hat{x}-z_f)+\hat{x}m_{J/\psi}^2)^2} \times 128Q^3\hat{x}^2m_{J/\psi}^2\Big(Q^4(-1+\hat{x})^2z_f^2+2m_{J/\psi}^2Q^2(-1+\hat{x})\hat{x}z_f(-1+6z_f-6z_f^2+2z_f^3) + m_{J/\psi}^4\hat{x}^2(-2+10z_f-11z_f^2+4z_f^3)\Big), \tag{A28}$$

$$\sigma_9^{N4} = -\frac{128Q^2P_T\hat{x}^3m_{J/\psi}^4(Q^2z_f[-1+4z_f-2z_f^2+\hat{x}(5-10z_f+4z_f^2)]+m_{J/\psi}^2\hat{x}(2-5z_f+2z_f^2))}{z_f^2[Q^2(-1+\hat{x})+\hat{x}m_{J/\psi}^2]^3[Q^2(1+\hat{x}-z_f)+\hat{x}m_{J/\psi}^2]^2}. \tag{A29}$$

6. Hard cross sections of $N(Ax,-(1-A)x)$ in (28)

$$\sigma_1^{N5} = \frac{1}{(1-z_f)z_f^2[Q^2(-1+\hat{x})+\hat{x}m_{J/\psi}^2]^3[Q^2(1+\hat{x}-z_f)+\hat{x}m_{J/\psi}^2]^3} \times 256Q^2P_T\hat{x}^3m_{J/\psi}^2\Big(2Q^6(-1+\hat{x})^2z_f(1-4z_f+2z_f^2)+m_{J/\psi}^2Q^4(z_f^2(-10+17z_f-12z_f^2+3z_f^3) - 2\hat{x}z_f(16-79z_f+108z_f^2-62z_f^3+13z_f^4)+2\hat{x}^2(-2+23z_f-84z_f^2+107z_f^3-59z_f^4+12z_f^5)) + m_{J/\psi}^4Q^2\hat{x}(2z_f(12-20z_f+13z_f^2-3z_f^3)+\hat{x}(30-149z_f+210z_f^2-123z_f^3+26z_f^4)) + m_{J/\psi}^6\hat{x}^2(-14+23z_f-14z_f^2+3z_f^3)\Big), \tag{A30}$$

$$\sigma_2^{N5} = \frac{1}{(1-z_f)z_f^2[Q^2(-1+\hat{x})+\hat{x}m_{J/\psi}^2]^3[Q^2(1+\hat{x}-z_f)+\hat{x}m_{J/\psi}^2]^3} \times 512Q^4P_T\hat{x}^3(-2+z_f)m_{J/\psi}^2\Big(Q^4(-1+\hat{x})^2z_f^2+2m_{J/\psi}^2Q^2(-1+\hat{x})\hat{x}z_f(-2+11z_f-12z_f^2+4z_f^3) + m_{J/\psi}^4\hat{x}^2(-4+20z_f-23z_f^2+8z_f^3)\Big), \tag{A31}$$

$$\sigma_3^{N5} = \frac{-1}{z_f^3[Q^2(-1+\hat{x})+\hat{x}m_{J/\psi}^2]^3[Q^2(1+\hat{x}-z_f)+\hat{x}m_{J/\psi}^2]^3} \times 128Q^3\hat{x}^2m_{J/\psi}^2\Big(Q^6(-1+\hat{x})^2z_f^2[3-3z_f+\hat{x}(-5+4z_f)]+m_{J/\psi}^2Q^4\hat{x}z_f[-4-43z_f+106z_f^2-80z_f^3+20z_f^4 - 4\hat{x}(1-39z_f+79z_f^2-55z_f^3+13z_f^4)+\hat{x}^2(8-113z_f+210z_f^2-140z_f^3+32z_f^4)] + m_{J/\psi}^4Q^2\hat{x}^2[z_f(100-221z_f+163z_f^2-40z_f^3)+\hat{x}(12-166z_f+321z_f^2-222z_f^3+52z_f^4)] + m_{J/\psi}^6\hat{x}^3(-52+114z_f-83z_f^2+20z_f^3)\Big), \tag{A32}$$

$$\sigma_4^{N5} = \frac{-1}{z_f^2(Q^2(-1+\hat{x})+\hat{x}m_{J/\psi}^2)^3(Q^2(1+\hat{x}-z_f)+\hat{x}m_{J/\psi}^2)^3} \times 256Q^2P_T\hat{x}^3(-2+z_f)m_{J/\psi}^4\Big(Q^4z_f[3(-1+z_f)z_f+2\hat{x}^2(2-7z_f+4z_f^2)-2\hat{x}(1-7z_f+5z_f^2)] + m_{J/\psi}^2Q^2\hat{x}[2(4-3z_f)z_f+\hat{x}(3-17z_f+10z_f^2)]+m_{J/\psi}^4\hat{x}^2(-5+3z_f)\Big), \tag{A33}$$

$$\sigma_8^{N5} = \frac{-1}{z_f^3(Q^2(-1+\hat{x})+\hat{x}m_{J/\psi}^2)^3(Q^2(1+\hat{x}-z_f)+\hat{x}m_{J/\psi}^2)^3} \times 128Q^3\hat{x}^2m_{J/\psi}^2\Big(Q^6(-1+\hat{x})^2(1+\hat{x}-z_f)z_f^2+m_{J/\psi}^2Q^4\hat{x}z_f[z_f(-9+22z_f-16z_f^2+4z_f^3) + \hat{x}^2(-4+17z_f-14z_f^2+4z_f^3)-4\hat{x}(-1+2z_f+2z_f^2-3z_f^3+z_f^4)] + m_{J/\psi}^4Q^2\hat{x}^2[z_f(12-35z_f+29z_f^2-8z_f^3)+\hat{x}(-4+10z_f+3z_f^2-10z_f^3+4z_f^4)] + m_{J/\psi}^6\hat{x}^3(-4+14z_f-13z_f^2+4z_f^3)\Big), \tag{A34}$$

$$\sigma_9^{N5} = \frac{256Q^2P_T\hat{x}^3(-2+z_f)(1-z_f)m_{J/\psi}^4(Q^4z_f(2\hat{x}^2+z_f-2\hat{x}z_f)+m_{J/\psi}^2Q^2\hat{x}(\hat{x}-2z_f+2\hat{x}z_f)+m_{J/\psi}^4\hat{x}^2)}{z_f^2[Q^2(-1+\hat{x})+\hat{x}m_{J/\psi}^2]^3[Q^2(1+\hat{x}-z_f)+\hat{x}m_{J/\psi}^2]^3}. \tag{A35}$$

[1] A. Adare *et al.* (PHENIX Collaboration), Phys. Rev. Lett. **103**, 012003 (2009); Phys. Rev. D **79**, 012003 (2009); L. Adamczyk *et al.* (STAR Collaboration), Phys. Rev. D **86**, 032006 (2012); P. Djawotho (STAR Collaboration), Nuovo Cimento Soc. Ital. Fis. **036C**, 35 (2013); A. Adare *et al.* (PHENIX Collaboration), Phys. Rev. D **90**, 012007 (2014).

[2] D. de Florian, R. Sassot, M. Stratmann, and W. Vogelsang, Phys. Rev. Lett. **113**, 012001 (2014).

[3] A. Accardi, J. L. Albacete, M. Anselmino, N. Armesto, E. C. Aschenauer, A. Bacchetta, D. Boer, W. K. Brooks, T. Burton, N. B. Chang *et al.*, Eur. Phys. J. A **52**, 268 (2016).

[4] R. D. Klem, J. E. Bowers, H. W. Courant, H. Kagan, M. L. Marshak, E. A. Peterson, K. Ruddick, W. H. Dragoset, and J. B. Roberts, Phys. Rev. Lett. **36**, 929 (1976).

[5] G. Bunce *et al.*, Phys. Rev. Lett. **36**, 1113 (1976).

[6] X. Ji, J. W. Qiu, W. Vogelsang, and F. Yuan, Phys. Lett. B **638**, 178 (2006).

[7] X. Ji, J.-W. Qiu, W. Vogelsang, and F. Yuan, Phys. Rev. D **73**, 094017 (2006).

[8] Y. Koike, W. Vogelsang, and F. Yuan, Phys. Lett. B **659**, 878 (2008).

[9] A. Bacchetta, D. Boer, M. Diehl, and P. J. Mulders, J. High Energy Phys. 08 (2008) 023.

[10] F. Yuan and J. Zhou, Phys. Rev. Lett. **103**, 052001 (2009).

[11] J. Zhou, F. Yuan, and Z. T. Liang, Phys. Rev. D **81**, 054008 (2010).

[12] J. W. Qiu, X. P. Wang, and H. Xing, Chin. Phys. Lett. **38**, 041201 (2021).

[13] M. Anselmino, M. Boglione, U. D'Alesio, E. Leader, and F. Murgia, Phys. Rev. D **70**, 074025 (2004).

[14] R. M. Godbole, A. Kaushik, and A. Misra, Phys. Rev. D **94**, 114022 (2016).

[15] U. D'Alesio, F. Murgia, C. Pisano, and P. Taels, Phys. Rev. D **96**, 036011 (2017).

[16] R. M. Godbole, A. Kaushik, and A. Misra, Phys. Rev. D **97**, 076001 (2018).

[17] U. D'Alesio, C. Flore, F. Murgia, C. Pisano, and P. Taels, Phys. Rev. D **99**, 036013 (2019).

[18] R. M. Godbole, A. Kaushik, A. Misra, and V. S. Rawoot, Phys. Rev. D **91**, 014005 (2015).
[19] A. Mukherjee and S. Rajesh, Eur. Phys. J. C **77**, 854 (2017).
[20] S. Rajesh, R. Kishore, and A. Mukherjee, Phys. Rev. D **98**, 014007 (2018).
[21] H. Sun, Tichouk, and X. Luo, Phys. Rev. D **100**, 014007 (2019).
[22] U. D'Alesio, F. Murgia, C. Pisano, and P. Taels, Phys. Rev. D **100**, 094016 (2019).
[23] R. Kishore, A. Mukherjee, and S. Rajesh, Phys. Rev. D **101**, 054003 (2020).
[24] U. D'Alesio, F. Murgia, C. Pisano, and S. Rajesh, Eur. Phys. J. C **79**, 1029 (2019).
[25] U. D'Alesio, L. Maxia, F. Murgia, C. Pisano, and S. Rajesh, Phys. Rev. D **102**, 094011 (2020).
[26] Z. B. Kang and J. W. Qiu, Phys. Rev. D **78**, 034005 (2008).
[27] Z. B. Kang, J. W. Qiu, W. Vogelsang, and F. Yuan, Phys. Rev. D **78**, 114013 (2008).
[28] H. Beppu, Y. Koike, K. Tanaka, and S. Yoshida, Phys. Rev. D **82**, 054005 (2010).
[29] Y. Koike and S. Yoshida, Phys. Rev. D **84**, 014026 (2011).
[30] H. Beppu, Y. Koike, K. Tanaka, and S. Yoshida, Phys. Rev. D **85**, 114026 (2012).
[31] Y. Koike, K. Yabe, and S. Yoshida, Phys. Rev. D **101**, 054017 (2020).
[32] P. J. Mulders and J. Rodrigues, Phys. Rev. D **63**, 094021 (2001).
[33] X. D. Ji, Phys. Lett. B **289**, 137 (1992).
[34] D. Boer, P. J. Mulders, and F. Pijlman, Nucl. Phys. **B667**, 201 (2003).
[35] Z. B. Kang, J. W. Qiu, W. Vogelsang, and F. Yuan, Phys. Rev. D **83**, 094001 (2011).
[36] R. b. Meng, F. I. Olness, and D. E. Soper, Nucl. Phys. **B371**, 79 (1992).
[37] W. E. Caswell and G. P. Lepage, Phys. Lett. **167B**, 437 (1986).
[38] G. T. Bodwin, E. Braaten, and G. P. Lepage, Phys. Rev. D **51**, 1125 (1995); **55**, 5853(E) (1997).
[39] U. D'Alesio, L. Maxia, F. Murgia, C. Pisano, and S. Rajesh, J. High Energy Phys. 03 (2022) 037.
[40] A. Schafer and J. Zhou, Phys. Rev. D **88**, 014008 (2013).
[41] S. Yoshida and D. Zheng, Phys. Rev. D **106**, 034019 (2022).
[42] F. Yuan, Phys. Rev. D **78**, 014024 (2008).
[43] U. A. Acharya *et al.* (PHENIX Collaboration), Phys. Rev. Lett. **127**, 162001 (2021).
[44] N. J. Abdulameer *et al.* (PHENIX Collaboration), Phys. Rev. D **107**, 052012 (2023).